Polymer 52 (2011) 3956–3962

Contents lists available at ScienceDirect

Polymer

journal homepage: www.elsevier.com/locate/polymer

Unexpected new phase detected in FT30 type reverse osmosis membranes using scanning transmission X-ray microscopy

Gary E. Mitchell [a,*], Bill Mickols [b], Daniel Hernandez-Cruz [c,1], Adam Hitchcock [c]

[a] Analytical Sciences, Dow Chemical, 1897 Bldg, Midland, MI 48667, USA
[b] Water & Process Solutions, Dow Chemical Company, 5230 West 73rd St., Minneapolis, MN 55439, USA
[c] Brockhouse Institute for Materials Research, McMaster University, Hamilton, ON L8S 4M1, Canada

ARTICLE INFO

Article history:
Received 16 February 2011
Received in revised form
28 June 2011
Accepted 2 July 2011
Available online 13 July 2011

Keywords:
Reverse osmosis membranes
X-ray microscopy
Poly phenylene diamine

ABSTRACT

FT30 type thin film composite membranes used for reverse osmosis water purification are very difficult to analyze. With the remarkably thin polyamide layer and surface modification of the polymers now being reported, a new analytical technique is needed to determine the surface structure and chemical distribution in the active layer. In this study we show that scanning transmission X-ray microscopy (STXM) can be used to determine the spatial distribution of polyamide and polysulfone and we report on the detection of an unexpected new phase. The new phase was identified as a homopolymer of the meta-phenylene diamine (MPD) that forms in MPD solutions and can be incorporated into the discrimination layer during the interfacial reaction with the TMC to produce a mixed polyamide polyMPD layer. The detection of this second phase was only made possible by STXM. At the levels detected in membranes in this study (less than 8%) the second phase had no effect on the flux or salt passage of the membranes, however at higher levels a change in the membrane properties most likely would occur and the quantity of the polyMPD present should be eliminated or controlled.

1. Introduction

The best reverse osmosis (RO) membranes for purification of water currently use the so-called FT30 thin film composite membrane patented by Cadotte in 1981 [1]. The FT30 type membranes are made in three layers (see Fig. 1). The first layer consists of a polyethylene terepthalate (PET) paper-like support and provides the mechanical strength to move the forming membrane through a complex process and to increase the strength of the ultrathin aromatic polyamide which needs to operate in excess of 1000 psi for seawater membranes. The second layer is a porous polysulfone, grown over the PET using a diffusion induced phase segregation process to form the pores, which are larger at the polyester interface and smaller at the top. This layer provides a scaffold on which to synthesize the third layer. Finally a layer of polyamide is grown on top of the polysulfone by interfacial polymerization. This third layer is very thin and provides the discrimination between water and solutes. This is the layer that does all the reverse osmosis. To produce this layer an amine functionalized monomer (usually meta-phenylene diamine; MPD) is dissolved in water and placed on the polysulfone and an acid chloride multifunctional monomer (usually trimesic acid chloride; TMC) dissolved in an organic solvent is flowed on top, so that reaction between the two monomers can occur at the water–oil interface. This process is quite elegant as it self-limits to a certain thickness as the diffusion of the amine to the reaction site becomes inhibited by the growing membrane. Likewise reaction continues at any pinholes until they are closed. The resulting polyamide layer is approximately 100 nm thick.

Analysis of the polyamide discrimination layer is challenging because of its thinness and its insolubility. Scanning and transmission electron microscopies (SEM and TEM) have been used successfully to characterize membranes [2,3], but these techniques do not provide chemical bonding information. In this paper we describe the use of soft X-ray Scanning Transmission X-ray Microscopy (STXM) [4,6] to analyze FT30 membranes. X-ray microscopy is an emerging analytical technology that has proven to be very useful for analysis of polymers which have chemical and physical heterogeneity at the sub micron size scale [4,5]. STXM uses soft X-ray near edge X-ray absorption fine structure (NEXFAS) spectral transitions as a contrast mechanism to provide visualization of the structure and quantitative analysis [6]. Chemical

* Corresponding author.
E-mail address: gemitchell001@gmail.com (G.E. Mitchell).
[1] Present address: Faculty of Engineering, Universidad Autonoma de Chiapas, Chiapas, CP 29000, Mexico.

0032-3861/$ – see front matter © 2011 Elsevier Ltd. All rights reserved.
doi:10.1016/j.polymer.2011.07.001

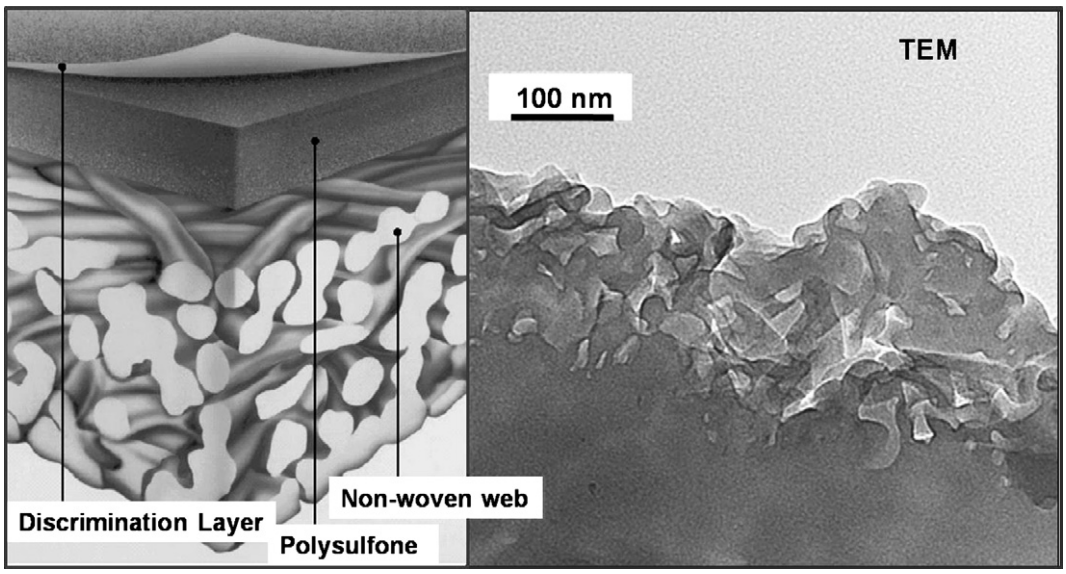

Fig. 1. Structure of an FT30 type RO Membrane.

bonding specific analysis can be performed at the resolution of the microscope (30 nm in our case) [7] and can be performed in 3 dimensions by using angle resolved tomography [8]. For TEM with a captive parallel energy loss spectrometer there is the potential for bonding information from the electron energy loss (EELS) spectrum, however it is difficult to get as high spectral resolution with TEM-EELS as with the use of soft X-rays in STXM [9]. Relative to TEM, STXM causes much less sample damage for an equivalent core level spectral analysis [18].

In order to analyze the multiple layers found in modern thin film composites, we chose to use STXM for its ability to differentiate chemical bonding and to generate images of the spatial distribution of different polymer phases. Modern membranes may be coated multiple times during their manufacture. The final (top) layer may be designed to provide enhanced rejection or better fouling resistance. Over the past several years Dow Water and Process Solutions has introduced a number of very high rejection membranes and there are also numerous reports of surface modification of RO membranes in the literature [3,10]. During our work to develop a STXM method to characterize the polymer layers and differentiate their spectra, we discovered an interesting new phase present in the polyamide layer of some membranes, which we have determined to be due to incorporation of homopolymers of one of the monomers (MPD) in the discrimination layer. The homopolymerization takes place in solution prior to the interfacial polymerization with TMC.

2. Experimental details

2.1. Materials

Reverse osmosis membranes were supplied by FilmTec Corporation (5230 W. 73rd St. Minneapolis, MN 55435). The FT30 membranes labeled BW30, which were commercial products produced prior to 2009, only contained the reaction products of 1,3-phenylene diamine with 1,3,5 benzene tri acid chloride and were not coated. The hand-made FT30 membranes were made in the laboratory. To hand make membranes, a portion of a porous polysulfone support was equilibrated in an aqueous 1,3-phenylene diamine solution (2.5% wt/wt). The support was removed from the aqueous solution and placed on a glass plate. The final droplets of MPD solution were removed from the surface and a 5 mM TMC solution in dodecane was applied to a level of about 5 mm. This was allowed to react for 1 min. The dodecane solution was removed and a rinse of hexane was used to remove unreacted acid chlorides. The membrane was then hung vertically to drain away and evaporate the excess hexane. This final membrane was then stored in water until used.

The oxidized MPD solution was prepared by mixing hydrogen peroxide into the 2.5% MPD at 0.01% (wt/wt). This was allowed to react for 1 h before the membrane was made using the oxidized MPD solution.

Cross sections were prepared by the following method: The membrane was peeled from the polyester layer and placed between two thin epoxy blocks for support. Thin cross sections ($\sim$100 nm) of the membranes were microtomed at room temperature, collected and placed on support grids. The grids were SiO coated 300 mesh thin bar copper transmission electron microscopy (TEM) grids from Ladd Research Company (83 Holly Court, Williston, VT 05495). The specimen then consisted of the polysulfone layer with polyamide layer attached. Often, the polyamide layer was not well attached to the polysulfone layer and would be lost during the sample preparation process. Using a vibrating diamond knife gave better detail for the pores in the polysulfone layer, but made no apparent difference for the polyamide layer.

For plan view samples, the polyamide discriminating layers were isolated using a method similar to that used in Ref. [11]. The polyamide and polysulfone layers of the membrane were removed from the polyester layer and sandwiched between two pieces of fine stainless steel screen. The samples were then immersed in dimethyl formamide (DMF) to dissolve the polysulfone. They were removed from the DMF and the mesh was opened up in a deionized water bath. As pieces of the membrane floated off they were collected and placed on 200 mesh uncoated copper TEM support grids.

A concentrated solution of polymerized MPD particles was made by aging a 3 wt% MPD solution of MPD dissolved in water for several days. This solution was passed through a Nalgene filter housing containing 0.1 μ filter paper (GE MAGNA, Nylon, Supported, Plain, 47 mm, R01SP04700). The filtration continued for several hours until the filter paper accumulated sufficient particles to stop the flow. The filter cake was too hard and tightly bound to

the surface of the paper to dislodge without scraping. Consequently, the dots of filter cake were scraped into 10 mL of MPD solution, creating a concentrated solution of MPD particles. For analysis in the STXM, a microliter drop of the particle rich solution was placed onto a Si_3N_4 window (100 nm thick) and allowed to dry.

Trimesic acid was obtained from Sigma–Aldrich (482749) at 95% purity. It was used without further purification by dissolving in toluene (1% by weight). A 1 μl drop was placed on a 100 nm thick Si_3N_4 membrane (Silson Ltd. JBJ Business Park, Northampton Road, Blisworth, Northampton, NN7 3DW, England). After the toluene had evaporated a thin film of trimesic acid remained. Spectra were measured from areas that were approximately 1 optical density (OD) thick at the most intense transition. Spectra of pure MPD (Sigma–Aldrich; P23954) were obtained in a similar way, except that the MPD was dissolved in water. Nomex™ was purchased as a pressed sheet of fibers (Goodfellow Metals; Ermine Business Park, Huntingdon, England PE29 6WR; cat # 980-751-00) 1 mm thick and was microtomed into sections of about 100 nm thickness (1.2 optical density units at 285 eV) and placed on a standard 200 mesh copper grid.

2.2. XRM instrumentation

The X-ray spectromicroscopy analyses were performed using the scanning transmission X-ray microscope (STXM) on beamline 5.3.2.2 at the Advanced Light Source at Lawrence Berkeley National Laboratory. This instrument has been described previously in Refs. [12,13]. X-rays produced by the bending magnet are energy selected by the spherical grating monochromator (resolution ~3000 E/ΔE; 50 μm entrance slit and 25 μm for the vertical and horizontal exit slits), focused onto the sample with Fresnel zone plate optics (25 nm outer zone width) and the transmitted X-rays are down-shifted into the visible by a thin phosphor screen and detected using a photomultiplier tube operated in photon counting mode. The sample is scanned in x and y using piezo-ceramic positioning to build up an image on a pixel by pixel basis. A two-dimensional differential interferometry system used in control mode ensures reproducible X-ray − sample positioning with 10 nm accuracy and a response time of ~100 Hz. The optimal spatial resolution is determined by the zone plate dimensions (Rayleigh resolution, $\delta = 1.22 \cdot$width of outer most zone, or 31 nm in the work reported here). Spectra may be obtained in microprobe fashion by pointing the beam at a spot of interest and scanning the wavelength, or defocusing the X-ray beam to cover a larger area. For this study, an image (or a single line) was acquired at different energies giving a spectrum at each pixel. The latter spectral acquisition methods are called spectral image stacks and linescan spectra (for the case where only a single line is repeatedly scanned instead of a 2 dimensional image) [8]. The incident intensity (I_0) was measured by including a region with a hole in the sample in the image stack area. The energy scale was calibrated within ±0.05 eV relative to the C 1s → 3s CO_2 peak at 292.74 eV [14]. A N_2 gas filter (1 m path length at 0.8 torr) was used to lessen higher energy X-rays coming from second order diffraction from the monochromator.

2.3. XRM data analysis methodology

After converting the spectral image stacks to optical density using a suitable I_0, they were converted to sets of component maps by fitting the spectrum at each pixel to the spectra of the three unique phases, using singular value decomposition (SVD) [7]. The software used was aXis2000 ver 25-Mar-05 and is publicly available freeware [15]. The methodology and the software used for this analysis are discussed by Koprinarov et al. [7]. These methods assume the spectrum at each pixel is a linear combination of the pure component spectra. They also assume that the spectra vary linearly with concentration (obey Beer–Lambert's law) and that the pure spectra for all components are included as input to the calculation.

3. Results

3.1. Cross sections

Fig. 2 shows two sets of composition maps derived from C 1s image stacks (as described above) for two different areas of a membrane analyzed (top versus bottom row). The three images at the left in each row are the composition of polysulfone, and two different phases detected in what should be the homogeneous polyamide layer of the membrane. The lighter the pixel the higher the level of that phase exists at any pixel. Conversely where any pixel is black it means that none of that phase was detected in the pixel. The fourth image from the left in each row is a pseudo color overlay of the first three images. The spectra used for the fitting were extracted by trial and error from pixels in the image stacks themselves, in locations selected to coincide with the polysulfone and polyamide layers. Two different sorts of spectra were found in

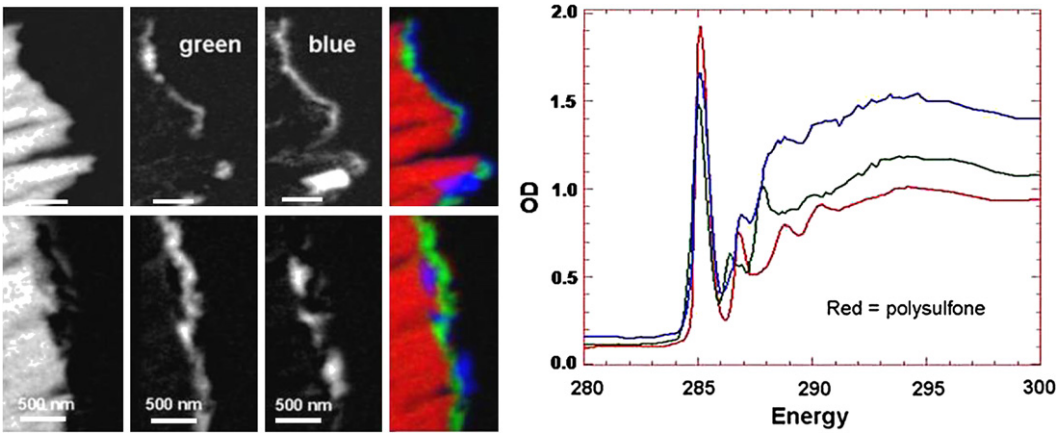

Fig. 2. Results from STXM C 1s image stack analyses of two different regions of a BW30 membrane. The spectra in the graph at right were extracted from selected areas of these images and used to calculate the composition maps shown for the top set. The red spectrum in each case indicates the polysulfone layer. The blue and green layers are different phases of the polyamide coating.

the polyamide layer, which was expected to be a single chemical species. The quality of the fit was improved by the following iterative procedure: The three spectra originally extracted from images manually were used to fit the data measured at each pixel. The composition maps thus generated were then used to generate regions of interest corresponding to each species by keeping only pixels above a certain value in each map (threshold masking). These regions of interest were then used to generate new spectra which were more representative of each phase (less contamination of the spectra with spectra from any adjoining phase). These new spectra were subsequently used to generate the image maps presented in Fig. 2.

3.2. Plan view

The thickness of the discrimination layer in FT30 membranes is fortuitously about one absorption length for the strongest peaks at the C 1s edge. By removing the polyamide layer from the polyester and the polysulfone layers, STXM can be used to obtain images in plan view. Fig. 3 shows results from curve fitting a plan view image stack using the spectra obtained from the cross section imaging in Fig. 2. The spectra recovered from the matrix and the particle phases of Fig. 3 were found to be identical to the spectra from the cross section analyses in Fig. 2 of the two phases in the polyamide layer. The composition map at the left indicates that this phase forms a matrix and is the dominant phase in the discrimination layer. The 2nd phase particles (blue) appear to be spherical. In the cross section images (Fig. 2) they seem of a different shape. An explanation for this could be that the microtome cuts for some cross sections may have been located across rows of particles. Additionally the polymer making up the second phase is apparently soft and was deformed and smeared by the microtoming. In the monochrome composition map at left, the black circles (black because none of the matrix phase is present in these pixels) correspond to the presence of the 2nd phase in the middle image. This indicates that the 2nd phase protrudes through the entire thickness of the discrimination layer. This makes sense since, if they are indeed spheres, their diameters are generally larger than the thickness of the discrimination layer, as judged from the images in Fig. 2 ($\sim$200 nm).

3.3. Spectroscopy

The C 1s NEXAFS spectra of MPD, trimesic acid, and poly-1,3-phenylene diamine isophthalic acid (Nomex®) were measured separately as reference spectra to help in identification of the phases in the discrimination layer. These spectra are presented in Fig. 4 along with the spectra of the two phases detected in the image stacks in Fig. 2. All three of the reference material spectra have a prominent peak near 285 eV which can be associated with an electronic transition from the C 1s orbital to the lowest unoccupied valence orbital, which is the $\pi^*_{C=C}$ molecular orbital on the aromatic ring [4,16,17]. In the case of the diamine, the $\pi^*;_{C=C}$ peak for the C atoms bonded to the N atoms occurs at 286.6 eV, because of stabilization of the 1s initial state orbital due to the electron withdrawing character of the N atom. The ratio of the integrated intensities of these two peaks should be directly proportional to the number of each type of carbon, that is 4:2 for 285.1–286.6 eV for MPD. There also could be some intensity due to transitions to the second ($\pi_2{}^*_{C=C}$) peak [16] for the four C atoms not bonded to N, that may distort the apparent ratio. The Nomex spectrum has a peak at 286.4 eV that can be likewise associated with the ring carbon atoms bonded to amide N atoms. The ratio of this peak to the one at 284.9 eV should be 2:10. For trimesic acid, there is most likely a resonant interaction between the $\pi^*;_{C=C}$ and the $\pi^*;_{C=O}$ orbitals through the aromatic electrons of the ring. This interaction causes the $\pi^*;_{C=C}$ band to move down in energy relative to its counterpart in the spectra of Nomex or MPD. This bond–bond interaction effect has been seen before for polyethylene terepthalate spectra [9]. Nomex has a main $\pi^*;_{C=C}$ peak energy between that for MPD and trimesic acid, which is consistent with it having both sorts of substituted phenyl rings. The peaks at 287.8 eV for Nomex and 288.2 eV for trimesic acid are attributed to C 1s(C=O) $\rightarrow$ $\pi^*;_{C=O}$ transitions at the carbonyl groups. The difference in energies of the carbonyl transitions can be explained by the difference in electron withdrawing power of amide NH versus the OH in the carboxylic acid group [18].

At the bottom of Fig. 4 the C 1s spectra of the two phases found in the discrimination layer are overlaid on the spectra of the reference compounds. The phase we have identified as polyamide matches very well with the Nomex spectrum. For the other phase, the only two bands that are obviously present are the two C 1s $\rightarrow$ $\pi^*;_{C=C}$ transitions at 285.2 and 286.9 eV. The higher one of the two ($\pi^*;_{N-\underline{C}=C}$) occurs at about 0.4 eV higher energy than the same band in the spectrum of MPD. The carbonyl band appears to be missing, although one cannot say this with total surety as there is a good deal of intensity at this spectral energy, just no well-defined peak.

To investigate the possibility that the new phase is derived from MPD homopolymer particles, we obtained samples of MPD solution from the FilmTec plant. The concentration of particles in the MPD application system is known to vary over time, depending upon the system residence time and the time since the last clean out. Samples of the MPD polymer particles for STXM analysis were

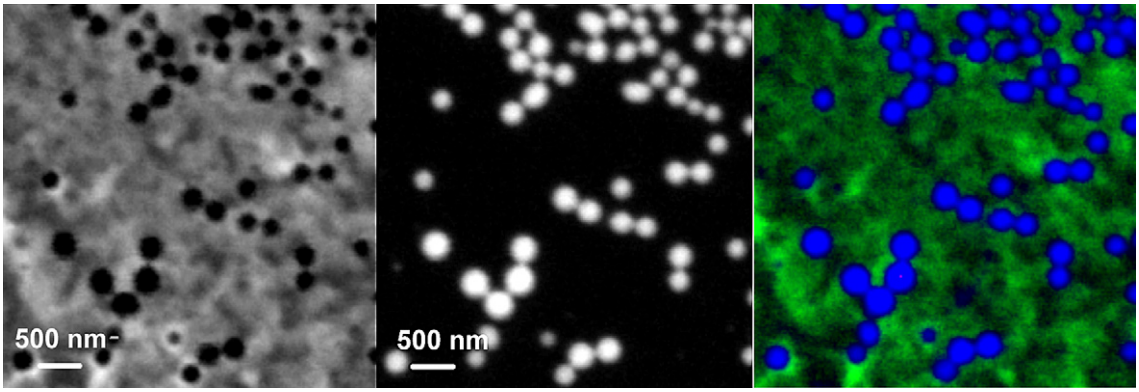

Fig. 3. Pixel–pixel curve fitting results for a BW30 membrane. At left and center are the two individual phases represented by green and blue in the colorized composition map on the right.

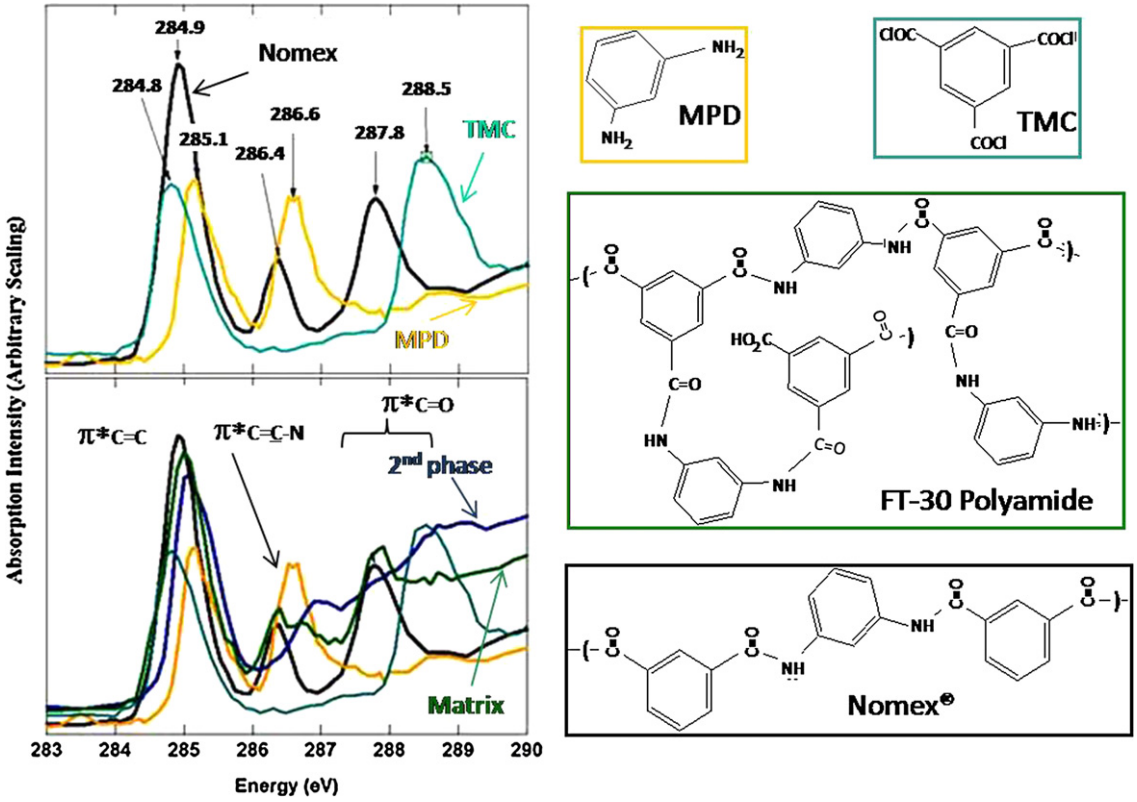

Fig. 4. Comparison of the spectra of Trimesic acid, 1,3-phenylene diamine and polyaramid to the spectra extracted from the two different phases detected in the polyamide layer of the membrane image stack reproduced in Fig. 2.

prepared as described above. Fig. 5 shows images and C 1s spectra of the particles and compares spectra of the polyMPD phase to a spectrum from some particles. The match is not perfect, but the spectra are very similar. The biggest difference is in the size and energy of the $\pi^*;_{N-C=C}$ band at 286.9 eV. For the 2nd phase in the discrimination layer, this peak is relatively smaller than that for the MPD polymer particles. TMC that dissolves or imbibes into the particles during the interfacial polymerization will at least partially react with free amine groups in the trapped MPD particles. The TMC will also form bonds to the outside of the particles which will serve to bind them into the polyamide layer. There would probably be excess carboxylic acid groups where the acid chloride did not react with amine, but was hydrolyzed. In Fig. 5 the 2nd phase spectrum does indeed have a peak at the same energy (288.5 eV) as the carbonyl peak from trimesic acid (Fig. 4). Note that the spectra of the 2nd phase in Fig. 5 came from a different sample than that in Fig. 4. There were small differences in the spectra for the 2nd phase from different samples and these differences should be expected. The spectral variations can be attributed to (1) differences in the exact history of the MPD solution from which the particles formed, and (2) differences in the amount of MPD or TMC imbibed into the particles. The size and shape of particles will also affect how much overlap there is between the matrix and the second phase in STXM images. This will affect how much the extracted spectra represent

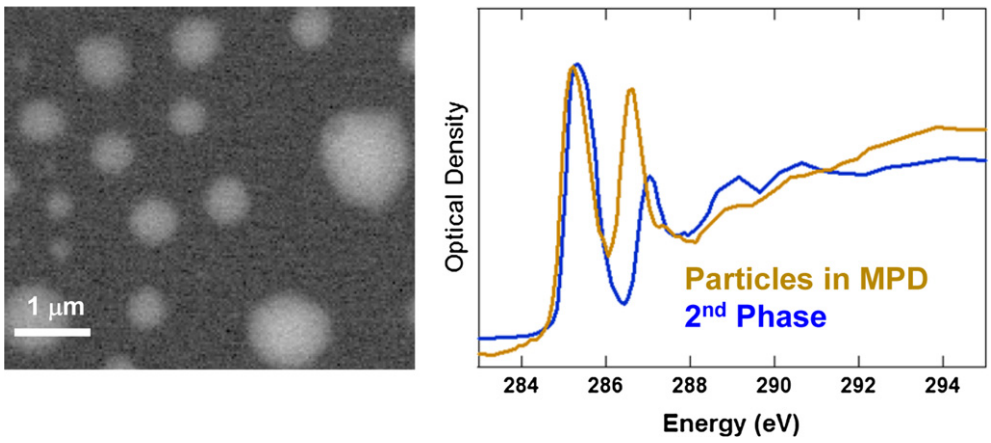

Fig. 5. On the left side is an image showing the particles harvested from the MPD solution and deposited on a 100 nm thick Si_3N_4 window. On the right is a comparison of the C 1s spectra of the MPD polymer particles with the blue phase. (For interpretation of the references to color in this figure legend, the reader is referred to the web version of this article.)

only the 2nd phase not contaminated with the spectrum from the adjacent polyamide. The uptake of TMC into the 2nd phase would decrease the relative number of free amine groups and also contribute more C=C carbon atoms that are not bonded to N atoms. Since the TMC has no electronegative nitrogen atom attached directly to the phenyl ring, the $\pi^*;_{N-\underline{C}=C}$ band would be smaller.

Finally, we note that the spherical particles appear to protrude through the entire discrimination layer thickness. This can be easily seen in the component maps reproduced on the left in Fig. 3. The location of the spheres in the center map of the new phase corresponds quite clearly to areas where there is zero intensity of polyamide phase in the left hand map.

MPD is known to polymerize oxidatively [19,20]. The particles may be polymerizing in solution by the effect of oxygen from the air. As a further test to confirm the identity of the 2nd phase, and test the effect on membrane properties, we purposely used hydrogen Peroxide to oxidize the MPD solution used to hand make membranes in the laboratory. Fig. 6 shows the STXM results for the membrane made with oxidized MPD. One notable observation from these data is that the particles in this membrane are not spherical but oddly shaped. Please note in Fig. 6 the left image is of standard polyamide and the center image is of the second phase with intensity distributed differently than the polyamide image. The right hand image shows that the polyamide (green) has a different distribution than the second phase (blue). A control membrane made with fresh MPD solution showed no evidence of the 2nd phase.

4. Discussion

One may wonder if the polyMPD particles can be detected by more conventional microscopies. We investigated this question using SEM and atomic force microscopy (AFM) to analyze membranes which STXM had determined to contain the polyMPD phase. The particles appeared to be visible in both SEM and AFM. However, after observing what was thought to be polyMPD particles in another membrane sample by SEM the analysis with STXM was unable to detect any of the additional phase. The reason for this discrepancy can be seen by referring to the excellent SEM and TEM article by Pacheco et al. [21]. Fig. 5 in their paper compares plan view images of the polyamide layer of an RO membrane by SEM and TEM. By careful observation it can be seen that what at first appears to be particles on the membranes are instead bubble-like structures in the polyamide. These sorts of features can also be seen in cross section TEM images [2,21]. Nonetheless, the polyMPD particles seem to be fairly common in FT30 type membranes and we have detected them in commercial membranes from other manufacturers. In searching the literature for other potential instances where the polyMPD particles have been unknowingly detected, we came across an article by Dutta et al. [22]. These researchers used infrared spectroscopy, positron annihilation lifetime spectroscopy, wide angle X-ray scattering and TEM to characterize the microstructure of neat, interfacially polymerized polyamide membrane material. They prepared their materials with varying MPD/TMC ratios and detected differing amounts of crystallinity in them that did not correlate with the MPD/TMC ratio. Using TEM and electron diffraction they detected dense, crystalline polymer particles non-uniformly distributed in at least one of their samples. These particles (Fig. 5a in Ref. [22]) appear quite similar to the polyMPD particles that we have identified here. Whether, or not they are the same cannot be determined from the conclusively. It is possible that their experimental procedures allowed the MPD solutions to age differently such that polyMPD particles were produced in some cases and not in others.

It is well known that particles form in MPD solutions, most likely from oxidative polymerization of the MPD molecules into a polyaniline homopolymer [19,20]. These particles will have residual amine groups at the surface as well as in their bulk and the amine groups would react with the TMC and with the forming polyamide layer during the interfacial polymerization process. This would thus trap them by covalently bonding into the discrimination layer, displacing polyamide that would otherwise form at the location of the polyMPD spheres.

Early on, one hypothesis regarding the identity of the newly discovered phase was that they were oligomers of TMC and MPD or internal salts of these oligomers. It is well known that oligomers of TMC and MPD become insoluble at very low degree of polymerization [23]. The hypothesis involved the formation of oligomers during the interfacial polymerization process that then became trapped in the polyamide layer. In order to test this hypothesis, several oligomers of this sort were made and spectra of these were measured. All of these materials gave C 1s spectra that were much more like the polyamide phase than the other phase. None of the C 1s spectra of these materials was a match for that of the polyMPD phase.

Possible structures for polymers of MPD have been described in the literature [24–26]. The ladder-like structure involving phenazine bonding between rings can be ruled out from the spectrum of polyMPD recorded for Fig. 5. For the latter structure the intensity ratio for $\pi^*;C=C$ near 285 eV to the $\pi^*;C=\underline{C}-N$ peak near 286.5 eV would be 2:4 which is clearly not the case. We did not specifically study the formation of the particles in MPD solutions or perform any other spectroscopy on the polyMPD. In this study the presence of the polyMPD particles in the discrimination layer had no measurable effect on either the salt passage or the flux. However it would be surprising if the polyMPD had exactly the same rejection

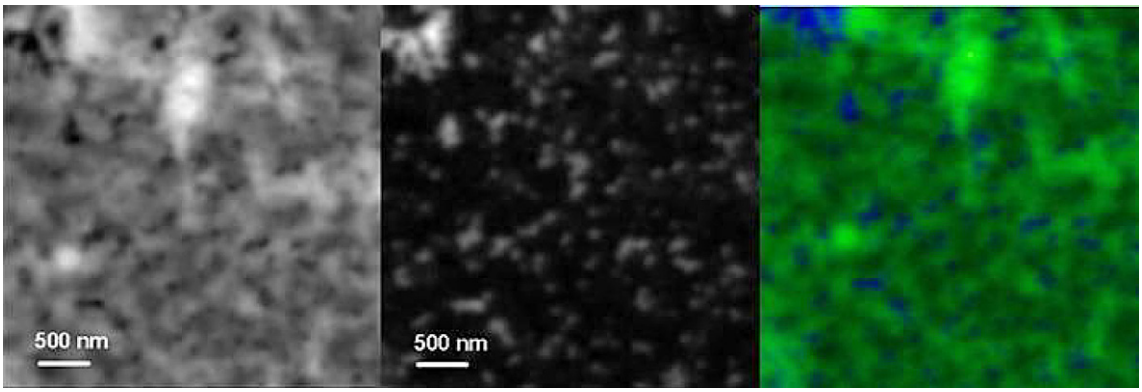

Fig. 6. STXM characterization of the polyamide discrimination layer for a membrane made with oxidized MPD. The map for the polyamide phase is on the left. At the center is a map for the 2nd phase and at the right is a colorized sum of the other two.

or flux characteristics as the polyamide. In the cases where the polyMPD particles do protrude through the entire polyamide film thickness, they are necessarily thicker than the polyamide and since they are thicker, the flux would be expected to decrease, even if the polyMPD had slightly higher flux than the polyamide. For this change in flux to be measurable requires that the number of particles were high enough to occupy a significant proportion of the surface area. The highest loading of the polyMPD particles that we encountered occupied an area of 8% of the membrane surface (that was imaged) as determined from the holes in the polyamide images (Fig. 3). The area of surface analyzed was only about 16 μm^2 and areas surrounding had less dense particle packing. Thus the true loading of the polyMPD was probably lower. Since good manufacturing practices call for eliminating inconsistency, it is a good idea to eliminate or control the quantity of the polyMPD present. It is certainly important to assure that the level of particles present in the discrimination layer stays low enough to have no measurable influence on flux or salt passage.

5. Conclusions

FT30 type thin film composites are very difficult to analyze. With the remarkably thin polyamide layer and surface modification of the polymers now being reported a new analytical technique is needed to determine the surface structure and chemical distribution in the active layer of the FT30 polymer. In this study we show that STXM can be used to determine the spatial distribution of polyamide and polysulfone as well as detecting an unexpected new phase. The new phase was identified as a homopolymer of the MPD that can be included in the interfacial reaction with the TMC to produce a mixed polyamide polyMPD layer. The presence of the polyMPD phase does not seem to matter at the levels detected, however at higher levels a change in the membrane properties most likely would occur and the quantity of the polyMPD present should be eliminated or controlled.

Acknowledgments

The X-ray microscopy was performed on beamline BL5.3.2.2 at the Advanced Light Source at Berkeley National Laboratory. The Advanced Light Source is supported by the Office of Basic Eenrgy Sciences of the Department of Energy, under contract DE-AC03-76SF00098. We would like to thank Mark Young for supplying the initial samples of the MPD particles. We owe a debt of gratitude to David Kilcoyneand Tolek Tyliszczak for their excellent support of the BL5.3.2.2 beamline.

References

[1] Cadotte J.E. U.S. Patent 4,277,344 (July 7, 1981).
[2] Cahill David G, Freger Viatcheslav, Kwak Seung-Yeop. MRS Bulletin 2008;33:27–32.
[3] Tang Chuyang Y, Kwon Young-Nam, Leckie James O. Journal of Membrane Science 2007;287(1):146–56.
[4] Ade Harald, Urquhart Stephen. NEXAFS spectroscopy and microscopy of natural and synthetic polymers. In: T.K. Sham pte. Ltd, editor. Chemical applications of synchrotron radiation. River Edge, NJ: World Scientific Publishing Company; 2002.
[5] Ade H, Hitchcock AP. Polymer 2008;49(3):643–75.
[6] Urquhart SG, Hitchcock AP, Smith AP, Ade HW, Lessard B, Lidy W, et al. Journal of Electron Spectroscopy and Related Phenomena 1999;100(1–3):119–35.
[7] Koprinarov IN, Hitchcock AP, McCrory C, Childs RF. Journal of Physical Chemistry B 2002;106(21):5358–64.
[8] Hitchcock AP, Johansson GA, Mitchell GE, Keefe MH, Tyliszcak T. Applied Physics A 2008;92(3):447–52.
[9] Rightor E, Hitchcock A, Ade H, Leapman R, Urquhart S, Smith A, et al. Spectromicroscopy of poly(ethylene terephthalate): comparison of spectra and radiation damage rates in X-ray absorption and electron energy loss. Journal of Physical Chemistry B 1997;101(11):1950–60.
[10] Sarkar Abhijit, Carver Peter I, Zhang Tracy, Merrington Adrian, Bruza Kenneth J, Rousseau Joseph L, et al. Journal of Membrane Science 2010;349(1–2):421–8.
[11] Freger Viatcheslav. Environmental Science and Technology 2004;38(11):3168–75.
[12] Ade H, Hitchcock AP, Mitchell GE, Kilcoyne ALD, Tyliszczak T, Fink R, et al. Synchrotron Radiation News 2003;16(3):53–63.
[13] Kilcoyne ALD, Tyliszczak T, Steele WF, Fakra S, Hitchcock P, Franck K, et al. Journal of Synchrotron Radiation 2003;10(2):25–136.
[14] Prince KC, Vondracek M, Karvonen J, Coreno M, Camilloni R, Avaldi L, et al. Journal of Electron Spectroscopy and Related Phenomena 1999;101–103:141–7.
[15] Axis is freeware written by Adam Hitchcock at McMaster University and is described and available at the following link: http://unicorn.mcmaster.ca/aXis2000.html.
[16] Stohr Joachim. NEXAFS spectroscopy. Springer-Verlag; June 1, 1996.
[17] Dhez O, Ade H, Urquhart SG. Journal of Electron Spectroscopy and Related Phenomena 2003;128(1):85–96.
[18] Urquhart SG, Ade H. Journal of Physical Chemistry B 2002;06(34):8531–8.
[19] Kennedy Brendan, Glidle Andrew, Cunnane Vincent J. Journal of Electroanalytical Chemistry 2007;608(1):22–30.
[20] Li Xin-Gui, Huang Mei-Rong, Duan Wei, Yang Yu Liang. Novel multifunctional polymers from aromatic diamines by oxidative polymerizations. Chemical Reviews 2002;102(9):2925–3030.
[21] Pacheco Federico A, Pinnau Ingo, Reinhard Martin, Leckie James O. Journal of Membrane Science 2010;358:51–9.
[22] Dutta D, Bhattacharyya A, Ganguly BN. Journal of Membrane Science 2003;224:127–35.
[23] Fiori Stefano, Monticelli Orietta, Alzari Valeria, Mariani Alberto. Journal of Applied Polymer Science 2010;115(6):3155–60.
[24] Sulimenko Tetyana, Stejskal Jaroslav, Proke Jan. Journal of Colloid and Interface Science 2001;236(2):328–34.
[25] Ichinohe Daigo, Muranaka Toshitaka, Sasaki Toshiya, Kobayashi Masami, Kise Hideo. Journal of Polymer Science: Part A: Polymer Chemistry 1998;36(14):2593–600.
[26] Ichinohe Daigo, Saitoh Norihiro, Kise Hideo. Macromolecular Chemistry and Physics 1998;199(6):1241–5.